

**Long-term pig manure application increases SOC through aggregate protection and Fe-C associations in a subtropical Red soil (Udic Ferralsols)**

Hui Rong<sup>a</sup>, Zhangliu Du<sup>b</sup>, Weida Gao<sup>a</sup>, Lixiao Ma<sup>c</sup>, Xinhua Peng<sup>d</sup>, Yuji Jiang<sup>e</sup>, Demin Yan<sup>f</sup>, Hu Zhou<sup>a</sup>

<sup>a</sup> Key Laboratory of Arable Land Conservation (North China), Ministry of Agriculture, College of Land Science and Technology, China Agricultural University, Beijing, China

<sup>b</sup> College of Resources and Environmental Sciences, China Agricultural University, Beijing 100193, China

<sup>c</sup> State Key Laboratory of Vegetation and Environmental Change, Institute of Botany, Chinese Academy of Sciences, Beijing 100093, China.

<sup>d</sup> Institute of Agricultural Resources and Regional Planning, Chinese Academy of Agricultural Sciences, Beijing 100081, China

<sup>e</sup> College of Resources and Environment, Fujian Agriculture and Forest University, Fuzhou, 350002, China.

<sup>f</sup> College of Criminal Science and Technology, Nanjing Police College, Nanjing 210023, China.

**Correspondence:** Hu Zhou (zhouhu@cau.edu.cn)

**Abstract**

Manure is known to improve soil organic carbon (SOC) in Fe-rich red soils, but the underlying stabilization mechanisms remain poorly understood. A long-term field experiment was conducted with four treatments: no amendment (Control), low manure (LM, 150 kg N ha<sup>-1</sup> yr<sup>-1</sup>), high manure (HM, 600 kg N ha<sup>-1</sup> yr<sup>-1</sup>), and high manure with lime (HML, 600 kg N ha<sup>-1</sup> yr<sup>-1</sup> plus 3000 kg Ca (OH)<sub>2</sub> ha<sup>-1</sup> 3yr<sup>-1</sup>). The quantity and quality of SOC were characterized by physical fractionation, <sup>13</sup>C NMR spectroscopy and thermogravimetry (TG) analysis from 0-20 cm depth. Manure application increased total SOC by 65.1%-126.7%, with the increase primarily occurring in the particulate organic matter (POM) fraction. Specifically, POM C increased substantially by 208%-592%, compared to a 32.0% -66.8% increase in MAOM C. POM C was stabilized through the process of hierarchical aggregation. Fresh manure inputs acted as binding nuclei, leading to an increase in macroaggregates (>0.25 mm) concurrently with a reduction in microaggregates (0.05–0.25 mm), physically isolating labile C from microbial decomposition. Concurrently, manure amendments triggered Fe-mediated chemical stabilization. The elevated pH (4.8 to 5.4-7.1) in the manure treatments enhanced non-crystalline Fe oxide (Fe<sub>o</sub>) content by 25.4%, which positively correlated with MAOM C ( $R^2 = 0.56$ ,  $P < 0.05$ ). Despite chemical composition shift toward aliphaticity and

reduced aromaticity, thermally stable organic matters increased by 8%–12%, revealing the critical role of Fe<sub>o</sub> in offsetting inherent molecular lability when aggregate protection was removed by destruction prior to TG analysis. Overall, this study proposes a dual SOC stabilization framework via physical and chemical Fe-carbon associations in a subtropical red soil.

**Keywords:** Particulate organic matter; Mineral-associated organic matter; Nuclear magnetic resonance; Thermogravimetry analysis

## 1. Introduction

Soil organic carbon (SOC), the largest carbon reservoir in the terrestrial ecosystems, plays critical roles in climate mitigation and soil multifunctionality (Amelung et al., 2020; Lal, 2004). Red soils (Udic Ferralsols, according to Chinese Soil Taxonomy) have low SOC content due to intense weathering and rapid mineralization in tropical and subtropical South China (Yan et al., 2013; Zhang et al., 2013). While manure has been widely used to enhance SOC in these soils (Bai et al., 2023; Nichitha et al., 2023; Zhang et al., 2023), the underlying mechanisms governing its stabilization remain elusive. Currently, the discrepancies existed regarding the manure-induced SOC accrual through chemical recalcitrance, physical protection (by aggregation processes), or organo-mineral interactions—given the Fe-enrich red soils and their pH-dependent reactivity (Kleber et al., 2021; Six et al., 2002; Song et al., 2022). Considering, the red soils covering 22% of China's cropland and low inherent SOC levels, it is essential to unveil Fe-C interactions that regulate SOC stabilization through organic amendments.

Existing studies showed some conflicting evidences on SOC stabilization pathways. For instance, Mustafa et al. (2021) reported increased aromatic C (chemically recalcitrant) with manure application, whereas Yan et al. (2013) observed preferential accumulation of labile O-alkyl C. This paradox highlighted uncertainties on how manure inputs altered SOC composition. It is reported that Fe oxides contributed to SOC stabilization in red soils (Zhang et al., 2013). These reactive Fe phases can form stable covalent bonds between their surface hydroxyls and organic functional groups, protecting SOC from microbial decomposition (Ruiz et al., 2024). In comparison with crystalline Fe oxides (Fe<sub>d</sub>), non-crystalline Fe oxides (Fe<sub>o</sub>) exhibit organic matter adsorption capacity primarily attributed to their larger specific surface area (Zhang et al., 2013). ~~The ratio of~~

~~Fe<sub>d</sub> and Fe<sub>o</sub> is dynamically regulated by pH, which can be intentionally manipulated through manure application (Liu et al., 2020; Wang et al., 2023). The long-term impacts of manure-induced pH shifts on Fe-oxide speciation and related organic carbon sequestration are still not well understood, despite the known connection between pH-driven Fe-oxide transformation and organic matter stabilization. Previous studies have demonstrated that long-term application of organic fertilizers—including manure, compost, and straw—significantly increased amorphous iron oxides (Fe<sub>o</sub>) in agricultural soils (Chen et al., 2022; Huang et al., 2018; Wang et al., 2019). These studies further revealed that redox cycling promoted the reductive dissolution of crystalline iron (Fe<sub>d</sub>), followed by its reprecipitation as amorphous Fe<sub>o</sub> during oxidative periods. On the other hand, soil pH was identified as a key factor dynamically influencing the Fe<sub>d</sub>/Fe<sub>o</sub> ratio (Liu et al., 2020; Wang et al., 2023). Although organic amendments are known to elevate pH in acidic red soils, the specific effect of soil pH modulating the formation and stabilization of Fe<sub>o</sub> remains unclear.~~ Additionally, previous studies widely isolated chemical recalcitrance, aggregation protection, or organo-mineral interactions separately, largely neglecting the integrative assessments including these pathways. To address this knowledge gap, an integrative approach combining physical fractionation, molecular characterization, and thermal stability analysis is essential for elucidating the coupled effects of manure on SOC quantity and quality.

Physically separating soil organic matter (SOM) into mineral-associated organic matter (MAOM) and particulate organic matter (POM) fractions could help to predict SOC dynamics, and clarify SOC stabilization mechanisms. The POM associated SOC (defined as POM C) physically protected in the macroaggregates, while MAOM associated SOC (defined as MAOM-C) chemically protected via organo-mineral bonding (Chenu et al., 2019; Lavalley et al., 2019; Poeplau et al., 2018). Although physical fractionation could effectively isolate operationally defined these SOC pools (Poeplau et al., 2018), it failed to reveal the chemical heterogeneity of SOC (Cotrufo et al., 2019; Lavalley et al., 2019). Thus, solid-state <sup>13</sup>C NMR spectroscopy could address this gap by quantifying SOC functional groups (e.g. alkyl, O-alkyl, aromatic C), after completely disrupting organo-mineral interaction by HF pretreatment (Kögel-Knabner, 1997). Additionally, the thermogravimetry (TG) could rapidly assess the thermal stability of SOC without requiring pretreatment (Gao et al., 2015). On the other hand, some advanced techniques such as nano-scale secondary ion mass spectrometry

(NanoSIMS) and high-resolution mass spectrometry could identify the spatial visualization of organo-mineral associations and molecular characterization, these approaches heavily required complex instrumentation and are not cost-effective for the comparative analysis of multiple samples. Therefore, combined NMR with TG approaches to efficiently evaluate the chemical composition and thermal stability of SOC in response to manure management.

The specific objectives of this study were: 1) to evaluate the changes of Fe oxides and its effect on MAOM formation; 2) to explore how soil aggregation affected POM formation; 3) to evaluate the effect of manure application on SOC composition and stability. We hypothesized that: 1) Manure application could enhance MAOM C formation by increasing non-crystalline Fe oxides ( $\text{Fe}_\text{o}$ ), induced by elevated pH; 2) Manure application would strengthen the physical protection due to the improved soil aggregation, which triggered labile SOC protection; 3) The application of pig manure would boost the recalcitrance of SOC, thus the thermal stability. ~~The specific objectives of this studies were: 1) to evaluate the changes of Fe oxides and its effect on MAOM formation; 2) to explore how soil aggregation affected POM formation; 3) to evaluate the effect of manure application on SOC composition and stability.~~

## 2. Materials and methods

### 2.1. Site description and experimental design

The long-term field experiment is located at Yingtan National Agroecosystem Field Experiment Station of the Chinese Academy of Sciences (28°15'20"N, 116°55'30"E) in Jiangxi Province, China. The site has a typically subtropical humid monsoon climate with a mean annual temperature of 17.6°C and precipitation of 1795 mm (Jiang et al., 2018). The soil is derived from Quaternary red clay, and is classified as Udic Ferralsols according to Chinese Soil Taxonomy. The soil contains 36.3% clay, 45.2% silt and 21.2% sand.

The field experiment was initiated in April, 2002. The soils used in this experiment were transported from adjacent forestland and repacked (to a depth of 2 m) for all the plots. This design ensures a uniform initial soil condition and eliminates the influence of prior land use history. Four treatments were compared: (1) no manure amendment (Control), (2) low pig manure with 150 kg N  $\text{ha}^{-1} \text{a}^{-1}$  (LM), (3) high pig manure with 600 kg N  $\text{ha}^{-1} \text{a}^{-1}$  (HM), and (4) high pig manure with 600

kg N ha<sup>-1</sup> a<sup>-1</sup> and lime (HML). The four treatments received solely pig manure as the nitrogen source, with no synthetic fertilizers applied. The pig manure, collected from nearby pig farms, contained an average total carbon of 386.5 g kg<sup>-1</sup>, total nitrogen of 36.2 g kg<sup>-1</sup> and total phosphorus of 21.6 g kg<sup>-1</sup> on a dry matter basis. The annual amount of pig manure applied to each treatment was calculated based on its nitrogen content. Since all aboveground residues (stalks and leaves) and manually recoverable roots were completely removed from the field after harvest, the total carbon inputs to the soil were derived ~~mainly~~exclusively from pig manure. This resulted in average annual carbon inputs of around 1.6 and 6.4 Mg C ha<sup>-1</sup> for the LM and HM treatments, respectively (see Supplementary Material for calculation details). The field experiment was set up following a completely randomized design, with each treatment has three replicate plots. ~~Each plot has a size of 2 m × 2 m.~~ Lime was applied at 3 000 kg Ca (OH)<sub>2</sub> ha<sup>-1</sup> (3a)<sup>-1</sup> for the HML treatment. The field was planted with corn (*Zea mays* L.) monoculture annually from April to July. The pig manure was applied annually each April onto the soil surface (0-10 cm depth) and subsequently incorporated into the topsoil through plowing and harrowing. All the management measures, including sowing, harvesting and weeding, were manually operated.

## 2.2 Sampling

Sampling was conducted in July 2019, after the harvest of corn. Triplicate topsoil samples (0-20 cm) were randomly collected with a shovel from each plot and composited together to form one bulk sample. The soil samples were air-dried at room temperature and were gently crushed with a rubber mallet to pass through an 8-mm sieve, preserving aggregates >8mm for further analysis. Visible plant residues, roots and stones were removed (Soil Survey Staff, 2011). No visible manure residues were observed.

## 2.3 Soil properties measurements

SOC and Total nitrogen (TN) were determined by an elemental analyzer (Vario MACRO, Elementar, Germany). Soil pH was measured using a glass electrode (PHS-3D, SANXIN, China) with soil: deionized water ratio of 1: 2.5. Crystalline (Fe<sub>a</sub>) and non-crystalline Fe oxides (Fe<sub>o</sub>) were extracted by DCB (Dithionite-citrate-bicarbonate) and oxalate, respectively (Yan et al., 2013), and then were determined by graphite furnace atomic absorption spectrometry (GFAAS) (PinAAcle 900T, PerkinElmer, America). Water stability of aggregates was tested using the fast-wetting method

following Le Bissonnais (1996). Aggregate stability was expressed as mean weight diameter (MWD). Detailed experimental processes and calculation can be found in Zhou et al. (2019).

#### 2.4. Physical fractionation

Soil was fractionated into MAOM (<53  $\mu\text{m}$ ) and POM (>53  $\mu\text{m}$ ) fraction following Cambardella and Elliott (1992) and Cotrofu et al. (2019). Briefly, 10 g sieved samples (<2 mm) were completely dispersed in dilute sodium hexametaphosphate (( $\text{NaPO}_3$ )<sub>6</sub>, 0.5%) at a soil: solution ratio of 1:4 by shaking for 18 h (25°C, 180 r min<sup>-1</sup>). This procedure primarily disrupts macroaggregates (>250  $\mu\text{m}$ ), but remaining that stable microaggregates (<53  $\mu\text{m}$ ). After dispersing, soil slurry was passed through a 53  $\mu\text{m}$  sieve and rinsed several times with deionized water. The fraction passing through the sieve was collected as MAOM fraction, and that remaining on the sieve was collected as POM fraction. Both fractions were centrifuged and the solution was decanted, and then the remaining material was oven-dried to constant weights at 60°C. SOC concentration of each fraction was measured using the wet oxidation method. Dried mass proportions of each fraction (g fraction g<sup>-1</sup> soil) were calculated as follows:

$$f_M = m_M / m_{bulk} \quad (1)$$

$$f_P = m_P / m_{bulk} \quad (2)$$

where  $f_M$  and  $f_P$  were the dried mass proportions of MAOM and POM fraction (g fraction g<sup>-1</sup> bulk soil), respectively;  $m_M$  and  $m_P$  (g) were the dried masses of MAOM and POM fractions;  $m_{bulk}$  (g) was the dried mass of bulk soil.

SOC in the MAOM and POM fractions were called as MAOM C and POM C, respectively in this paper. MAOM C and POM C were calculated by multiplying the dried mass proportions of each fraction (g fraction g<sup>-1</sup> soil) by the respective SOC concentrations (g C kg<sup>-1</sup> fraction) as follows (Garten and Wulfschleger, 2000; Lian et al., 2015):

$$\text{MAOM C} = f_M \times \text{SOC}_M \quad (3)$$

$$\text{POM C} = f_P \times \text{SOC}_P \quad (4)$$

where  $f_M$  and  $f_P$  were calculated by Equation (1) and Equation (2);  $\text{SOC}_M$  and  $\text{SOC}_P$  were the SOC concentrations in the MAOM and POM fraction (g C kg<sup>-1</sup> fraction), respectively.

The contributions of MAOM C and POM C to total SOC (%) was calculated as:

$$\text{Contribution of MAOM C (\%)} = \text{MAOM C} / \text{Total SOC} \times 100 \quad (5)$$

$$\text{Contribution of POM C (\%)} = \text{POM C} / \text{Total SOC} \times 100 \quad (6)$$

where MAOM C and POM C were derived from Equations (3) and (4), respectively; total SOC was the content of SOC in the bulk soil.

## 2.5. SOC chemical composition and chemical stability

SOC chemical composition was analyzed with a solid-state cross-polarization magic angle spinning (CPMAS)  $^{13}\text{C}$  nuclear magnetic resonance (NMR) spectroscopy. Prior to NMR analysis, <2 mm air-dried soils were pretreated with hydrofluoric acid (HF) to remove paramagnetic  $\text{Fe}^{3+}$  (iron oxides) following Gao et al. (2021). While HF pretreatment can dissolve short-range-order minerals and potentially disrupt certain organo-mineral associations, it is an essential step to improve the signal-to-noise ratio and spectral resolution required for the reliable quantification of carbon functional groups. Firstly, 20 g soil was mixed with 100 mL 10% (w/w) HF solution in a polyethylene bottle and then shaken for 0.5 h per day for three days. Afterwards, the supernatant liquid was discarded and another 100 mL 10% HF solution was added again. The above procedures were repeated for 15 times. The residue was rinsed 10 times with deionized water until the pH was close to neutral. The remaining soil was freeze-dried and then ground in an agate mortar to pass through a 100-mesh sieve (0.149 mm) for further analysis. This fine grinding ensured homogeneous packing in the NMR rotor, minimizing signal heterogeneity (Simpson & Simpson, 2012).

Carbon functional groups were determined with the Bruker Ascend 500 MHz NMR spectrometer (Bruker BioSpin, Rheinstetten, Germany). Dry powdered samples were placed in a 4-mm sample rotor operating at a  $^{13}\text{C}$  resonance frequency of 125.8 MHz. The NMR spectrometer run at a spinning rate of 5kHz, and 10500 scans were collected for each sample. The spectra were collected over an acquisition time of 12 ms and a recycle delay of 0.8 s. All obtained spectra were processed with phase and baseline corrections. To allow for a direct comparison of the relative distribution of carbon functional groups, the total spectral intensity of each spectrum was normalized to that of the control soil sample. The normalized spectra were then integrated across and we assigned the obtained spectra to four different carbon functional groups, i.e., alkyl C (0-45 ppm), O-alkyl C (45-110 ppm), aromatic C (110-160 ppm) and carbonyl C (160-220 ppm) according to Kögel-Kanbner (1997). The relative concentrations of the different functional groups were calculated as the percentage of their peak areas to the total areas using MestReNova 14.0 software (Mestrelab Research, 2019, Spain).

Indices used to evaluate SOC recalcitrance include: alkyl C/O-alkyl C, aromaticity, aromatic C/O-alkyl C, aliphatic C/aromatic C and aliphaticity (Baldock et al., 1997; Du et al., 2017). Aromaticity = aromatic C / (alkyl C + O-alkyl C + aromatic C); Aliphatic C = alkyl C + O-alkyl C; Aliphaticity = (alkyl C + O-alkyl C) / (alkyl C + O-alkyl C + aromatic C). The alkyl C/O-alkyl C ratio reflects the degree of microbial transformation, with higher values indicating advanced decomposition and accumulation of recalcitrant alkyl compounds (Baldock et al., 1997). The aromatic C/O-alkyl C ratio aligns with the alkyl C/O-alkyl C ratio in reflecting the degree of SOC decomposition, whereas the aliphatic C/aromatic C ratio presents a contrary perspective to them. Aromaticity is a chemical concept denoting the resistance to microbial degradation (Kögel-Knabner, 1997). Aliphaticity is used to quantify the proportion of labile aliphatic components relative to stable aromatic moieties.

## 2.6. Thermogravimetry analysis

TG analysis was performed using a Netzsch TG 209F1 (Netzsch-Gerätebau GmbH, Selb, Germany). Air-dried soil samples were first sieved through a 2-mm mesh, and then ground in a ball mill to pass through a 50  $\mu\text{m}$  sieve. The grounded soil samples (5 ~ 10 mg) were placed in an  $\text{Al}_2\text{O}_3$  crucible covered with an aluminum lid and were oxidized in an atmosphere of 20  $\text{mL min}^{-1}$  of synthetic air (20%  $\text{O}_2$  and 80%  $\text{N}_2$ ) and 20  $\text{mL min}^{-1}$  of  $\text{N}_2$  as a protective gas. The temperature program included a heating rate of 10°C  $\text{min}^{-1}$  from 40°C up to 800°C. The sample mass percentage relative to the initial mass as a function of temperature was recorded simultaneously, and its first derivative (DTG) was calculated to represent the mass loss rate.

Three processes were detected in the temperature range of 40°C to 800°C: hygroscopic moisture evaporation, SOM decomposition and carbonate breaking down (Gao et al., 2015; Siewert, 2004). Based on the observed DTG curve, the weight loss between 180°C and 530°C, representing the temperature range during which SOM was decomposed, was defined as the total mass of SOM ( $\text{Exo}_{\text{tot}}$ ). The mass loss between 180°C and 380°C was a consequence of thermally labile SOM oxidation ( $\text{Exo}_1$ ) and that between 380°C and 530°C was caused by the combustion of more stable organic matter ( $\text{Exo}_2$ ) (Gao et al., 2015; Volkov et al., 2020). We used two parameters, the ratio of  $\text{Exo}_1$  and  $\text{Exo}_{\text{tot}}$  ( $\text{Exo}_1 / \text{Exo}_{\text{tot}}$ ) and the temperature at which half of the SOM was decomposed ( $\text{TG-T}_{50}$ ), to characterize the thermal stability of SOM. Higher  $\text{Exo}_1 / \text{Exo}_{\text{tot}}$  and lower  $\text{TG-T}_{50}$  values



indicate that the sample has more thermally labile or unstable SOM (Gao et al., 2015; Siewert, 2004).

## 2.7. Statistical analysis

Statistical analyses were carried out with R Studio software (R Development Core Team, version 4.1.2). One-way analysis of variance (ANOVA) was conducted to assess the effect of amendments on soil physico-chemical properties, SOC physical fractions, chemical composition and thermal indices. The independence of samples, normality of ~~residuals~~ ~~residues~~ and homogeneity of variances were checked by Chisq, Shapiro-Wilk and Bartlett test, respectively. Fisher's least significant difference (LSD) method was used for the multiple comparisons of means with a 0.05 significance level. Linear regression analysis was conducted to investigate the correlations between SOC and iron oxides, soil aggregation. Principal component analysis (PCA) was performed to evaluate the relationship between the quantity and quality of SOC and factors related to chemical protection and physical protection. Pearson correlation analyses were performed to explore the relationships between chemical composition and thermal indices.

## 3. Results

### 3.1. Long-term pig manure application increased SOC, TN, pH, non-crystalline ( $Fe_o$ ) and improved soil aggregation

Long-term manure amendment altered the soil ~~physico-chemical~~ ~~physic-chemical~~ properties (Table 1). ~~Relative to the Control, the SOC concentration was LM, HM and HML treatments increased SOC concentration by 64.9%, 116.2% and 126.6% higher in the LM, HM and HML treatments, respectively ( $P < 0.05$ ), and increased TN concentration by was 48.0%-108.2% higher ( $P < 0.05$ ). The pH values were increased by 0.62-2.28 units higher than those in the Control after pig manure application ( $P < 0.05$ ).~~ Application of pig manure had no significant effect on crystalline iron oxides ( $Fe_d$ ) content ( $P > 0.05$ ), but the HM and HML treatments ~~showed~~ significantly ~~greater increased~~ non-crystalline iron oxides ( $Fe_o$ ), ~~with an increase of by 25.4% relative to the Control ( $P < 0.05$ ).~~ ~~Relative~~ ~~Compared~~ to the Control, the HM and HML treatments ~~had~~ significantly ~~higher increased~~ macroaggregates ( $>0.25$  mm) content by 15.8% and 16.8%, respectively, and ~~they increased greater mean weight diameter (MWD) by 24.3% and 35.0%, respectively ( $P < 0.05$ ).~~ ~~In contrast, M~~ microaggregates (0.05-0.25 mm) was ~~decreased by 30.4% and 36.4%, respectively lower~~ under the HM and HML treatments, ~~with reduction of 30.4% and 36.4%, respectively ( $P < 0.05$ ).~~

### 3.2. Long-term pig manure application affected SOM physical fractions: MAOM and POM

The distribution of MAOM and POM fractions was significantly influenced by manure and lime amendments ( $P < 0.05$ , Table 2). Across all treatments, MAOM dominated the soil mass proportion (72.5%–75.1%), whereas ~~the proportion of POM was mass proportion increased~~ progressively ~~higher, ranging~~ from 16.6% in the ~~e~~Control to 19.3%–19.4% under the HM and HML treatments.

Manure application improved SOC concentration in both fractions, ~~SOC in the MAOM fraction was with increase rates of 32.0%-66.8% greater, and that in the POM fraction was 208%-592% greater relative to the Control~~ in the MAOM and POM fractions, respectively. ~~Despite this, The contribution of MAOM to total SOC was lower declined from 82.4% in the HM and HML treatments (65.5%-65.8%) than in the Ccontrol (82.4%) to 65.5%–65.8% under the HM and HML treatments, while the contribution of POM was contribution increased nearly threefold higher (increasing from 8.8% to 23.7%–26.0%).~~ Lime addition (HML vs. HM) did not significantly alter mass proportions but further enhanced POM C concentration (+15.4%) and its ~~contribution to total SOC-contribution~~ (+9.7%).

### 3.3. Effect of long-term pig manure application on SOC chemical composition and recalcitrance

The solid-state  $^{13}\text{C}$  NMR spectra showed different signal patterns for the different treatments (Fig. 1) and quantified the ratios of the different SOC functional groups shown in Table 3. Relative to ~~the~~ Control, the HM and HML treatments ~~had a significantly higher increased-proportion of~~ alkyl C by 4.6%–4.9% ( $P < 0.05$ ), while the LM treatment showed no significant ~~differencechange~~ ( $P > 0.05$ ). ~~The proportion of O-alkyl C was also significantly higher under the LM, HM and HML treatments, with increases of increased by 5.5%, 2.6% and 2.2% under the LM, HM and HML treatments, respectively ( $P < 0.05$ ). In contrast, the proportions of Aaromatic C and carbonyl C were lower in the manure-amended treatments, with reduction of decreased by 12.4%–13.2% and 0.9%–8.7%, respectively, in the manured treatment ( $P < 0.05$ ). While aromatic C was increased in the content after manure amend, its relative proportion was decreased by 12.4%–13.2% ( $P < 0.05$ ).~~

Relative to ~~the~~ Control, the ~~LM treatment significantly decreased~~ alkyl C/O-alkyl C ratio ~~was significantly lower under the LM treatment ( $P < 0.05$ )~~, ~~but~~ whereas the HM and HML treatments had no significant effect on the ratio ( $P > 0.05$ , Table3). The aromaticity was decreased by 14.4%, 12.9% and 13.2% under LM, HM and HML treatments, respectively ( $P < 0.05$ , Table3). Similarly,

the aromatic C/O-alkyl C ratio was decreased by 14.7%-17.7% lower in the manured treatment ( $P < 0.05$ , Table3). Conversely, both the aliphatic C/aromatic C ratio and aliphaticity were increased by 18.1%-20.7% and 2.44%-3.66% higher in the manured treatments, with elevations of 18.1%-20.7% and 2.44%-3.66%, respectively ( $P < 0.05$ , Table3).

### 3.4. The effect of long-term pig manure application on SOC thermal stability

The shapes of TG and its first derivatives (DTG) curves showed distinct weight losses rate as temperature increased to above 100°C, in the order of HM>HML>LM>Control (Fig. 2). Relative to the Control treatment, pig manure application significantly increased the total mass losses in the range of 180°C to 530°C ( $Exo_{tot}$ ) by 11.1%-17.4% ( $P < 0.05$ , Table 4), and significantly increased the mass losses during 180-380°C ( $Exo_1$ ) and 380-530°C ( $Exo_2$ ) by 14.6%-26.5% and 7.8%-13.7%, respectively ( $P < 0.05$ , Table 4). The LM and HML treatments significantly increased the ratio of  $Exo_1/Exo_{tot}$  was significantly elevated in the LM and HM treatments ( $P < 0.05$ ), whereas the HM treatment showed no significant effect relative to the Control ( $P > 0.05$ , Table 4). HM and HML treatments significantly decreased TG- $T_{50}$  by 10.7-12.0 °C ( $P < 0.05$ ), while LM treatments showed no significant difference compared to Control ( $P > 0.05$ , Table 4).

### 3.5. Relationships between SOC and factors related to the mineral protection and physical protection of SOC

Fig. 3 showed correlations between SOC and possible variables associated with the chemical protection and physical protection of SOC. SOC in the bulk soil was significantly positively correlated with MAOM C ( $R^2=0.97$ , Fig. 3A). MAOM C showed no relationship with  $Fe_d$  ( $R^2=0.04$ , Fig. 3B), it was positively correlated with  $Fe_o$  ( $R^2=0.56$ , Fig. 3C). A weaker correlation was observed between MAOM C and the content of clay and silt ( $R^2 = 0.34$ ,  $P = 0.46$ , Fig. 3D) there was no correlation between MAOM C and the content of clay and silt ( $R^2=0.34$ , Fig.3D). Notably,  $Fe_o$  concentration was significantly and positively correlated with pH ( $R^2=0.59$ ,  $P<0.01$ ; Fig. 4A). Conversely, the concentration of  $Fe_d$  was not correlated with pH ( $P>0.05$ ; Fig. 4B).

SOC in the bulk soil was significantly positively correlated with POM C ( $R^2=0.95$ , Fig. 3E). POM C was significantly associated with soil aggregation, evidenced by the positive correlation with macroaggregates ( $>0.25$  mm) ( $R^2=0.78$ , Fig. 3F) and MWD ( $R^2=0.67$ , Fig. 3H), while negative correlation with microaggregates ( $<0.25$  mm) ( $R^2=-0.71$ , Fig. 3G).

A PCA plot diagram (Fig. 54) revealed distinct associations between SOC quantity/quality and stabilization mechanisms. SOC vector aligned positively with POM C, macroaggregates and MWD, but inversely with microaggregates. Chemically, SOC covaried with MAOM C and Fe<sub>o</sub>, yet formed an obtuse angle (>90°) with Fe<sub>d</sub>. TG-T<sub>50</sub> negatively associated with the proportion of O-alkyl C and aliphaticity (angles > 90°), but positively linked to aromatic C and aromaticity (angles < 90°).

## 4. Discussion

### 4.1. POM C and physical protection

Long-term pig manure application caused an increase of SOC in the bulk soil relative to the Control, and the increase was mainly derived from continuous manure inputs (Gong et al., 2009). Although maize rhizodeposition (including root exudates and sloughed-off cells) (typically <10% of net primary productivity; Pausch and Kuzyakov, 2018) contributes to SOC during the growing season, its annual carbon inputs are only 0.2-0.5 Mg C ha<sup>-1</sup> yr<sup>-1</sup> (Dennis et al., 2010). This plant-derived C input is much lower than that from manure, contribution is negligible in comparison with manure inputs, which ranged from 1.6 to 6.4 Mg C ha<sup>-1</sup> yr<sup>-1</sup> in the LM and HM treatments, respectively. The rigorous removal of all harvest residues (stalks and recoverable roots) minimized excluded aboveground and root biomass as a source of soil carbon deposition. It should be noted that some residual plant-derived materials (e.g., fine root fragments and exudates) have contributed marginally to the SOC pool. Given the relatively small quantity of plant-derived carbon inputs, the changes in SOC observed in this study are primarily attributable to the application of pig manure. Thus, the SOC increase in the LM/HM treatments (Table 1) can be predominately attributed to the exogenous organic C supplied by pig manure, and the HML treatment can be partly influenced by lime. Following microbial decomposition and transformation, the applied manure-C was progressively partitioned into distinct SOC pools.

Manure-derived carbon was preferentially allocated to the POM fraction rather than the MAOM fraction. The contribution of POM C to SOC in the manure-amended treatment increased was nearly threefold as that in the Control (8.8% to 26.0%), while that the proportion of MAOM C decreased significantly from 82.4% in the Control to 65.4%–71.0% in the under manure application treatments (Table 2). The result was in line with Lan et al. (2022) and Li et al. (2018), who reported that increased manure substitution improved the POM C/MAOM C ratio, indicating manure was

beneficial to the formation of POM C. These results implied carbon inputs are preferentially stabilized as POM rather than MAOM. This finding is supported by biomarker evidence showing a great contribution of plant-derived carbon to the POM fraction (Zou et al., 2023). Consistent with this, a  $^{13}\text{C}$  isotopic tracing study revealed that 70%-87% of residue-derived SOC was accumulated in the POM fraction at two experimental sites (Mitchell et al., 2021). The mechanism behind this preferential sequestration is the physical occlusion of fresh organic material within macroaggregates, which provides initial protection against rapid microbial decomposition. Therefore, POM C can be a good indicator of SOC dynamics under field management (Álvaro-Fuentes et al., 2021; Wu et al., 2023). Recent biomarker evidence demonstrated that plant derived carbon contributes disproportionately to POM in comparison with MAOM fraction (Zou et al., 2023). Notably,  $^{13}\text{C}$  isotopic tracing study revealed that 70%–87% of residue-derived SOC was accumulated in the POM fraction at two sites in the study of Mitchell et al. (2021). These results jointly validate that fresh organic inputs are distributed primarily in the POM fraction due to direct occlusion within macroaggregates before microbial processing. Therefore, POM C can be a good indicator of SOC dynamics under field management (Álvaro-Fuentes et al., 2021; Wu et al., 2023).

While POM C is inherently labile and susceptible to decomposition, it can be physically protected from rapid decay through occlusion within stable soil aggregates. POM C was susceptible to decomposition due to its rapid dynamics, whereas it was simultaneously protected through physical occlusion within soil aggregates. According to the classical hierarchical aggregation model (Six et al., 2000), organic carbon acts as a primary binding agent for microaggregates (<0.25mm) to form macroaggregates (>0.25mm), with POM serving as both a structural nucleus and a transient carbon reservoir (Six et al., 2000). In this study, macroaggregates were significantly increased, and free microaggregates were significantly decreased after pig manure application (Table 1). These results implied that manure-derived carbon acted as binding agent, promoting the formation of macroaggregates from free microaggregates, bound microaggregates to form macroaggregates, thus This process provides physical protection for SOC, particularly that in the POM fraction, within the newly formed aggregates, providing physical protection for SOC particularly in the POM fraction (Peng et al., 2023). The observed positive correlation between POM C and both macroaggregates and aggregate MWD (Fig.3; Fig.4) further suggested verified the critical role of soil aggregation.

However, the physical mechanisms by which POM facilitates this process (e.g., microbial mediation, hydrophobic interactions, or polysaccharide bridging) require further investigation. Experimental approaches such as isotopic labelling combined with micro-scale imaging (e.g., electron microscopy or X-ray computed tomography) can visualize the spatial distribution of POM within aggregates and quantify its role in aggregate formation. Future study should pay attention to these new technologies.

#### 4.2. MAOM C and chemical protection

MAOM retained higher SOC concentrations (4.18-7.09 g C kg<sup>-1</sup> bulk soil) than the POM fraction did, irrespective of treatments, though its contribution to total SOC decreased after manure application (Table 2). MAOM C remained the dominant SOC reservoir, consistently comprising over 65% of the total SOC across all treatments (Table 2). This underscores that organo-mineral complexation, rather than physical protection within aggregates, is the primary stabilization pathway in these red soils, even under significant organic input. MAOM C exhibited significantly longer mean residence time (MRT) compared to POM C, with reported turnover periods of 26-40 years versus 2.4-4.3 years, respectively (Benbi et al., 2014; Garten and Wullschlegel, 2000). This fundamental difference originates from the unique stabilization mechanism of MAOM C through persistent organo-mineral associations (Lavalley et al., 2019). While clay minerals are widely recognized as key MAOM stabilizers (Hemingway et al., 2019; Liang et al., 2017), our study reveals a distinct iron oxide-dominated mechanism in these Fe-rich red soils. The strong correlation between MAOM C and non-crystalline Fe oxides (Fe<sub>o</sub>,  $R^2=0.56$ ; Figs. 3C, 4) highlighted the pivotal role of Fe<sub>o</sub> on SOC stabilization in this red soil. This iron-mediated stabilization likely stems from the exceptionally high specific surface area of Fe<sub>o</sub> (~800 m<sup>2</sup> g<sup>-1</sup> in ferrihydrite; Kleber et al., 2005) and its superior capacity to form stable organo-mineral complexes (Eusterhues et al., 2005; Lehmann and Kleber, 2015). Previous studies have demonstrated that organic amendments can enhance the content of non-crystalline Fe oxides, thereby promoting Fe-C associations (Chen et al., 2022; Huang et al., 2017; Wang et al., 2019). Extending these findings, our results provide new mechanistic insight by demonstrating that the increase in non-crystalline Fe oxides is closely linked to manure-induced soil alkalization. Specifically, the significant positive correlation between pH and Fe<sub>o</sub>

indicates that the ~~The~~ increased pH after manure application (Table 1) created conditions favoring Fe<sub>o</sub> preservation (Vithana et al., 2015), with an increase of 25.4% in the content of Fe<sub>o</sub>. The ~~higher~~ increased Fe<sub>o</sub> content provided abundant reactive surfaces for MAOM formation. ~~The nature of this interaction likely involves specific molecular-scale binding mechanisms. Recent advances in synchrotron-based spectroscopy (e.g., STXM-NEXAFS) have provided direct evidence that poorly crystalline iron oxides (e.g., ferrihydrite) stabilize organic carbon primarily through ligand exchange, where carboxyl (-COOH) and hydroxyl (-C-OH) functional groups in organic molecules replace the surface hydroxyl groups on Fe oxides (Ruiz et al., 2024). Furthermore, coprecipitation, where organic matter is encapsulated within the matrix of forming Fe (oxyhydr)oxides, represents another potent stabilization mechanism that can generate long-term sinks for organic carbon (Chen et al., 2014). While our bulk data cannot unequivocally distinguish between these mechanisms, the correlation suggests that similar processes are likely operative in our system, contributing to the stability of the large MAOM-C pool.~~ This pH-Fe<sub>o</sub>-MAOM nexus establishes a self-reinforcing stabilization mechanism: manure-derived organic ligands interact with Fe<sub>o</sub> to form stable complexes, simultaneously protecting both organic carbon and Fe<sub>o</sub> from dissolution (Kleber et al., 2021).

The positive correlation between Fe<sub>o</sub> and MAOM C (Fig. 3C) suggested that non-crystalline Fe oxides played a critical role in stabilizing SOC through organo-mineral interactions. However, while our data support the association between Fe<sub>o</sub> and MAOM C, the underlying mechanisms (e.g., adsorption, co-precipitation, or ligand exchange) remain speculative due to the lack of direct molecular-scale evidence. Future studies employing advanced spectroscopic techniques (e.g., synchrotron-based X-ray absorption spectroscopy or NanoSIMS) could explicitly characterize the binding forms of Fe-organic complexes, thereby validating the causal relationship between Fe<sub>o</sub> and MAOM formation.

#### 4.3. Chemical composition and thermal stability

Input of new organic material could alter chemical composition of SOC and lead to the change of the molecule recalcitrance of SOC (Guo et al., 2019; Yan et al., 2013; Zhou et al., 2010; Zhang et al., 2013). In the current study, pig manure application ~~resulted in a higher proportion~~ increased the ~~content~~ of O-alkyl C ~~but a lower proportion of aromatic C, but declined that of aromatic C.~~ ~~Given~~ ~~P~~ pig manure was rich in cellulose and lignin components, ~~so the its~~ introduction ~~of manure~~



~~greatly~~substantially increased O-alkyl C relative to the Control (Li et al., 2015). The considerable ~~accumulation~~increase of O-alkyl C accounted for the ~~reduction~~decrease of the relative proportion of aromatic C and the ~~decrease of~~lower aromaticity.

Long-term pig manure application strengthened SOC thermal stability by improving the content of thermally stable organic matters while it decreased TG-T<sub>50</sub>. The observed increase in the absolute amount of thermally stable SOC (Exo<sub>2</sub>) can be attributed to the formation of stable organo-mineral complexes with newly formed Fe<sub>o</sub>. As elucidated by Kleber et al. (2021), the thermal stability of organic matter is significantly enhanced upon binding to mineral surfaces. Thermal analysis suggested that manure amend significantly increased SOM content, evidenced by the increase of the mass losses during 180-530 °C (Exo<sub>tot</sub>) (Table 4). The result was consistent with the change of SOC content measured by conventional method (Table 1), indicating TG technology was promising for measuring SOM content (Siewert, 2004; Tokarski et al., 2018). The decrease of TG-T<sub>50</sub> reflected more easily decomposable SOC accumulated after manure application (Gao et al., 2015; Siewert, 2004). The result consisted with that in the NMR spectroscopy, where greater O-alkyl C and higher aliphaticity were found under manure treatments (Table 3). SOC with more O-alkyl C functional groups or higher aliphaticity was less likely to resist thermochemical degradation as revealed by the negative relationship between TG-T<sub>50</sub> and aliphaticity (Fig.4; Fig. 5) (Hou et al., 2019; Lehman and Kleber, 2015), thus leading to a decrease of TG-T<sub>50</sub>. In this study, the thermally labile organic matters accounted for over half of the total organic matters, so the decrease of TG-T<sub>50</sub> after manure application was just a result of the increased thermally organic matters not the decrease of thermal stability. In contrast, thermal stability should be strengthened according to the increased thermally stable organic matters after manure application. The observed decrease TG-T<sub>50</sub> and the simultaneous increase in Exo<sub>2</sub> are not contradictory. This apparent paradox can be explained by the dual effect of manure amendment: the input of a large quantity of labile, manure-derived organic compounds significantly increased the proportion of thermally labile C, thereby reducing the average stability of the entire SOM pool (as reflected by the decreased TG-T<sub>50</sub>). Concurrently, the manure-induced biogeochemical changes (e.g., increased pH and Fe oxide transformation) promoted the formation of highly stable organo-mineral complexes. While the relative proportion of this stable C might be diluted by the new labile C, its absolute amount within the soil system increased substantially, which



465 is captured by the increase in the absolute Exo<sub>2</sub> signal. Since soil structure was destroyed due to the  
466 ground process of soil samples before TG analysis, the increase of the thermally stable organic  
467 matters was ascribed to mineral protection, where the correlations between organic carbon and Fe  
468 oxides increased the thermally resistance of OC (Ruiz et al., 2023).

## 469 **5. Conclusion**

470 Manure application increased SOC quantity and improved its quality in Fe-rich red soils. SOC in  
471 the POM fraction exhibited the most pronounced response to manure inputs, while the majority of  
472 SOC was stored in the MAOM fraction. Furthermore, SOC was stabilized by distinct yet  
473 complementary mechanisms: physical protection via aggregation process, and chemical protection  
474 via Fe-organic associations induced by elevated pH. In addition, manure application increased  
475 thermally stable organic matters. However, to better understand inherent mechanisms, future work  
476 should focus on molecular-scale characterization of Fe-organic interactions using synchrotron  
477 techniques (e.g., Fe K-edge XANES/EXAFS), and in-situ visualization of POM-mediated  
478 aggregation through advanced imaging tools (e.g., SEM-TEM or  $\mu$ -CT) coupled with <sup>13</sup>C-labelled  
479 manure to track POM dynamics within aggregates.

## 481 **Acknowledgments**

482 This work was financially supported by the NSFC-CAS Joint Fund Utilizing Large-scale Scientific  
483 Facilities (No. U1832188) and Chinese Universities Scientific Fund (2023RC047). We thank  
484 Yanyan Cai and Xing Xia for laboratory assistance.

## 486 **Author contributions**

487 HR conceived the experimental approach, took soil samples from the field, carried out the laboratory  
488 and data analyses, wrote the first draft of the manuscript, and contributed to subsequent drafts. ZLD  
489 helped analyze NMR spectrum and revise the manuscript. WDG contributed to interpreting TG  
490 data and revising the manuscript. LXM conducted the experiment of NMR. XHP helped design the  
491 experiment, and analyze data. YJJ contributed to the design of field experiment and the process of  
492 taking soil samples. DMY contributed to the process of writing. HZ contributed to funding  
493 acquisition, conceiving the experimental approach, carrying out data interpretations, and the writing

of all subsequent manuscript drafts.

## Conflict of Interest

Hu Zhou is a member of the editorial board of SOIL.

## References

- Álvaro-Fuentes, J., Franco-Luesma, S., Lafuente, V., Sen, P., Usón, A., Cantero-Martínez, C., and Arrúe, J.L.: Stover management modifies soil organic carbon dynamics in the short-term under semiarid continuous maize, *Soil Till. Res.*, 213, 105143, <https://doi.org/10.1016/j.still.2021.105143>, 2021.
- Amelung, W., Bossio, D., de Vries, W., Kögel-Knabner, I., Lehmann, J., Amundson, R., Bol, R., Collins, C., Lal, R., Leifeld, J., Minasny, B., Pan, G., Paustian, K., Rumpel, C., Sanderman, J., van Groenigen, J.W., Mooney, S., van Wesemael, B., Wander, M., and Chabbi, A.: Towards a global-scale soil climate mitigation strategy. *Nat. Commun.*, 11, 5427, <https://doi.org/10.1038/s41467-020-18887-7>, 2020.
- Baldock, J.A., Oades, J.M., Nelson, P.N., Skene, T.M., Golchin, A., and Clarke, P.: Assessing the extent of decomposition of natural organic materials using solid-state <sup>13</sup>C NMR spectroscopy, *Soil Res.*, 35, 1061–1084, <https://doi.org/10.1071/S97004>, 1997.
- Bai, X.X., Tang, J., Wang, W., Ma, J.M., Shi, J., and Ren, W.: Organic amendment effects on cropland soil organic carbon and its implications: A global synthesis, *Catena.*, 231, 107343, <https://doi.org/10.1016/j.catena.2023.107343>, 2023.
- Benbi, D.K., Boparai, A.K., and Brar, K.: Decomposition of particulate organic matter is more sensitive to temperature than the mineral associated organic matter, *Soil Biol. Biochem.*, 70, 183-192, <https://doi.org/10.1016/j.soilbio.2013.12.032>, 2014.
- Cambardella, C.A., and Elliott, E.J.: Particulate soil organic-matter changes across a grassland cultivation sequence, *Soil Sci. Soc. Am. J.*, 5, 777-783, <https://doi.org/10.2136/sssaj1992.03615995005600030017x>, 1992.
- Chen, M., Zhang, S., and Liu, L.: Organic fertilization increased soil organic carbon stability and sequestration by improving aggregate stability and iron oxide transformation in saline-alkaline soil. *Plant Soil* 474, 233–249. <https://doi.org/10.1007/s11104-022-05326-3>, 2022.
- Chenu, C., Angers, D.A., Barre, P., Derrien, D., Arrouays, D., and Balesdent, J.: Increasing organic stocks in agricultural soils: Knowledge gaps and potential innovations, *Soil Till. Res.*, 188, 41-52, <https://doi.org/10.1016/j.still.2018.04.011>, 2019.
- Cotrufo, M.F., Ranalli, M.G., Haddix, M.L., Six, J., and Lugato, E.: Soil carbon storage informed by particulate and mineral-associated organic matter, *Nature Geosci.*, 12, 989-996, <https://doi.org/10.1038/s41561-019-0484-6>, 2019.
- Dennis, P.G., Miller, A.J., and Hirsch, P.R.: Are root exudates more important than other sources of rhizodeposits in structuring rhizosphere bacterial communities? *FEMS Microbiol Ecol.*, 72, 313-327, <https://doi.org/10.1111/j.1574-6941.2010.00860.x>, 2010.
- Eusterhues, K., Rumpel, C., and Kögel-Knabner, I.: Organo-mineral association in sandy acid forest soils: importance of specific surface area, iron oxides and micropores, *Eur. J Soil Sci.*, 56, 753-763, <https://doi.org/10.1111/j.1365-2389.2005.00710.x>, 2005.
- Gao, Q.Q., Ma, L.X., Fang, Y.Y., Zhang, A.P., Li, G.C., Wang, J.J., Wu, D., Wu, W.L., and Du, Z.L.: Conservation

tillage for 17 years alters the molecular composition of organic matter in soil profile, *Sci. Total Environ.*, 762, 143116, <https://doi.org/10.1016/j.scitotenv.2020.143116>, 2021.

Gao, W.D., Zhou, T.Z., and Ren, T.S.: Conversion from conventional to no tillage alters thermal stability of organic matter in soil aggregates, *Soil Sci. Soc. Am. J.*, 79, 585-594, <https://doi.org/10.2136/sssaj2014.08.0334>, <https://doi.org/10.1016/j.scitotenv.2020.143116>, 2015.

Garten, C.T., and Wullschlegel, S.D.: Soil carbon dynamics beneath switchgrass as indicated by stable isotope analysis, *J. Environ. Qual.*, 29, 645-653, <https://doi.org/10.2134/jeq2000.00472425002900020036x>, 2000.

Gong, W., Yan, X.Y., Wang, J.Y., Hu, T.X., and Gong, Y.B.: Long-term manure and fertilizer effects on soil organic matter fractions and microbes under a wheat–maize cropping system in northern China, *Geoderma*, 149, 318-324, <https://doi.org/10.1016/j.geoderma.2008.12.010>, 2009.

Guo, Z.C., Zhang, J.B., Fan, J., Yang, X.Y., Yi, Y.L., Han, X.R., Wang, D.Z., Zhu, P., and Peng, X.H.: Does animal manure application improve soil aggregation? Insights from nine long-term fertilization experiments. *Sci. Total Environ.*, 660, 1029-1037, <https://doi.org/10.1016/j.scitotenv.2019.01.051>, 2019.

Hemingway, J.D., Rothman, D.H., Grant, K.E., Rosengard, S.Z., Eglinton, T.I., Derry, L.A., and Galy, V.: Mineral protection regulates long-term preservation of natural organic carbon, *Nature*, 570, 2717-2726, <https://doi.org/10.1038/s41586-019-1280-6>, 2019.

Hou, Y.H., Chen, Y., Chen, X., He, K., and Zhu, B.: Changes in soil organic matter stability with depth in two alpine ecosystems on the Tibetan Plateau, *Geoderma*, 351, 153-162, <https://doi.org/10.1016/j.geoderma.2019.05.034>, 2019.

Huang, X., Feng, C., and Zhao, G.: Carbon Sequestration Potential Promoted by Oxalate Extractable Iron Oxides through Organic Fertilization. *Soil Sci. Soc. Am. J.* 81, 1359–1370. <https://doi.org/10.2136/sssaj2017.02.0068>, 2017.

Jiang, Y.J., Zhou, H., Chen, L.J., Yuan, Y., Fang, H., Luan, L., Chen, Y., Wang, X.Y., Liu, M., Li, H.X., Peng, X.H., and Sun, B.: Nematodes and microorganisms interactively stimulate soil organic carbon turnover in the macroaggregates, *Front Microbiol.*, 9, 2803, <https://doi.org/10.3389/fmicb.2018.02803>, 2018.

Kleber, M., Bourg, I.C., Coward, E.K., Hamsel, C.M., Myneni, S.C.B., and Nunan, N.: Dynamic interactions at the mineral-organic matter interface, *Nat. Rev. Earth Environ.*, 2, 402–421, <https://doi.org/10.1038/s43017-021-00162-y>, 2021.

Kleber, M., Mikutta, R., Torn, M.S., and Jahn, R.: Poorly crystalline mineral phases protect organic matter in acid subsoil horizons, *Eur. J. Soil Sci.*, 717-725, <https://doi.org/10.1111/j.1365-2389.2005.00706.x>, 2005.

Kögel-Knabner, I.: <sup>13</sup>C and <sup>15</sup>N NMR spectroscopy as a tool in soil organic matter studies, *Geoderma*, 80, 243-270, [https://doi.org/10.1016/S0016-7061\(97\)00055-4](https://doi.org/10.1016/S0016-7061(97)00055-4), 1997.

Lal, R.: Soil carbon sequestration impacts on global climate change and food security, *Science*, 304, 1623-1627, <https://doi.org/10.1126/science.1097396>, 2004.

Lan, Z.J., Shan, J., Huang, Y., Liu, X. M., Lv, Z.Z., Ji, J.H., Hou, H.Q., Xia, W.J., and Liu, Y.R.: Effects of long-term manure substitution regimes on soil organic carbon composition in a red paddy soil of southern China, *Soil Till. Res.*, 221, 105395, <https://doi.org/10.1016/j.still.2022.105395>, 2022.

Lavallee, J.M., Soong, J.L., Cotrufo, M.F.: Conceptualizing soil organic matter into particulate and mineral-associated forms to address global change in the 21st century, *Glob. Chang Biol.*, 26, <https://doi.org/10.1111/gcb.14859>, 2019.

Le, Bissonnais, Y.: Aggregate stability and assessment of soil crustability and erodibility: I. Theory and methodology, *Eur. J. Soil Sci.*, 47, 425-437, <https://doi.org/10.1111/j.1365-2389.1996.tb01843.x>, 1996.

Lehmann, J., Kleber, M.: The contentious nature of soil organic matter, *Nature*, 528, 60-68, <https://doi.org/10.1038/nature16069>, 2015.

- Li, J., Wen, Y., Li, X., Li, Y., Yang, X., Lin, Z., Song, Z., Cooper, J., and Zhao, B.: Soil labile organic carbon fractions and soil organic carbon stocks as affected by longterm organic and mineral fertilization regimes in the North China Plain, *Soil Till. Res.*, 175, 281–290, <https://doi.org/10.1016/j.still.2017.08.008>, 2018.
- Li, Z.Q., Zhao, B.Z., Wang, Q., Cao, X.Y., and Zhang, J.B.: Differences in chemical composition of soil organic carbon resulting from long-term fertilization strategies, *PLoS One*, 10, e0124359, <https://doi.org/10.1371/journal.pone.0124359>, 2015.
- Lian, T.X., Wang, G.H., Yu, Z.H., Li, Y.S., Liu, X.B., and Jin, J.: Carbon input from <sup>13</sup>C-labelled soybean residues in particulate organic carbon fractions in a Mollisol. *Biol. Fertil. Soils*, 52, 331–339, <https://doi.org/10.1007/s00374-015-1080-6>, 2015.
- Liang, C., Schimel, J.P., and Jastrow, J.D.: The importance of anabolism in microbial control over soil carbon storage, *Nat. Microbiol.*, 2, 1–6, <https://doi.org/10.1038/nmicrobiol.2017.105>, 2017.
- Liu, S. B., Wang, J.Y., Pu, S.Y., Blagodatskaya, E., Kuzyakov, Y., and Razavi, B. S.: Impact of manure on soil biochemical properties: A global synthesis, *Sci. Total Environ.*, 745, 141003, <https://doi.org/10.1016/j.scitotenv.2020.141003>, 2020.
- Mitchell, E., Scheer, C., Rowlings, D., Contrufo, F., Conant, R.T., and Grace, P.: Important constraints on soil organic carbon formation efficiency in subtropical and tropical grasslands, *Glob. Change Bio.*, 27, 5383–5391, <https://doi.org/10.1111/gcb.15807>, 2021.
- Mustafa A., Xu, H., Shah, S.A.A., Abrar, M.M., Maitlo, A.A., Kubar, K.A., Saeed, Q., Kamran, M., Naveed, M., Wang, B.R., Sun N., and Xu, M.G.: Long-term fertilization alters chemical composition and stability of aggregate-associated organic carbon in a Chinese red soil: evidence from aggregate fraction, C mineration, and <sup>13</sup>C NMR analyses, *J. Soil Sediment*, 21, 2483–2496, <https://doi.org/10.1007/s11368-021-02944-9>, 2021.
- Nichitha, C.V, Raghaven, S., Champa, B.V., Ganapathi, G., Sudarshan V., Nandita, S., Ravikumar, D., and Nagaraja, M.S.: Role of organic manures on soil carbon stocks and soil enzyme activities in intensively managemend ginger production systems. *Int. J. Recycl. Org. Waste Agric.*, 1579, <https://doi.org/10.30486/IJROWA.2023.1977064.1579>, 2023.
- Pausch, J., and Kuzyakov, Y.: Carbon input by roots into the soil: Quantification of rhizodeposition from root to ecosystem cell, *Global Change Biol.*, 24, 1–12, <https://doi.org/10.1111/gcb.13850>, 2018.
- Peng, X.Y., Huang, Y., Duan, X.W., Yang, H., and Liu J.X.: Particulate and mineral-associated organic carbon fractions reveal the roles of soil aggregates under different land-use types in a karst faulted basin of China, *Catena*, 220, 106721, <https://doi.org/10.1016/j.catena.2022.106721>, 2023.
- Poeplau, C., Don, A., Six, J., Kaiser, M., Benbi, D., Chenu, C., Cotrufo, M.F., Derrien, D., Gioacchini, P., Grand, S., Gregorich, E., Griepentrog, M., Gunina, A., Haddix, M., Kuzyakov, Y., Kühnel, A., Macdonald, L.M., Soong, J., Trigalet, S., Vermeire, M.-L., Rovira, P., van Wesemael, B., Wiesmeier, M., Yeasmin, S., Yevdokimov, I., and Nieder, R.: Isolating organic carbon fractions with varying turnover rates in temperate agricultural soils – A comprehensive method comparison, *Soil Biol. Biochem.*, 125, 10–26, <https://doi.org/10.1016/j.soilbio.2018.06.025>, 2018.
- Ruiz, F., Rumpel, C., Dignac, M-F., Baudin, F., and Ferreira, T. O.: Combing thermal analyses and wet-chemical extractions to assess the stability of mixed-nature soil orgnaic matter, *Soil Biol. Biochem.*, 187, 109216, <https://doi.org/10.1016/j.soilbio.2023.109216>, 2023.
- Ruiz, F., Bernardino, A. F., Queiroz, H. M., Otero, X. L., Rumpel, C., and Ferreira, T. O.: Iron’s role in soil organic carbon (de)stabilization in mangroves under land use change, *Nat. Commun.*, 10433, <https://doi.org/10.1038/s41467-024-54447-z>, 2024.
- Shi, R.Y., Liu, Z.D., Li, Y., Jiang, T.M., Xu, M.G., Li, J.Y., and Xu, R.K.: Mechanisms for increasing soil resistance

to acidification by long-term manure application, *Soil Till. Res.*, 185, 77-84,  
<https://doi.org/10.1016/j.still.2018.09.004>, 2019.

Siewert, C.: Rapid screening of soil properties using thermogravimetry, *Soil Sci. Soc. Am. J.* 68, 1656-1661,  
<https://doi.org/10.2136/sssaj2004.1656>, 2004.

Simpson, M.J., and Simpson, A.J.: The chemical ecology of soil organic matter molecular constituents, *J. Chem. Ecol.*, 38, 768–784, <https://doi.org/10.1007/s10886-012-0122-x>, 2012.

Six, J., Elliot, E.T., and Paustian, K.: Soil macroaggregate turnover and microaggregate formation: a mechanism for  
 C sequestration under no-tillage agriculture, *Soil Biol. Biochem.*, 32, 2099-2103,  
[https://doi.org/10.1016/S0038-0717\(00\)00179-6](https://doi.org/10.1016/S0038-0717(00)00179-6), 2000.

Six, J., Conant, R.T., Paul, E.A., and Paustian, K.: Stabilization mechanisms of soil organic matter: Implications for  
 C-saturated soils, *Plant Soil*, 241, 155-176, <https://doi.org/10.1023/A:1016125726789>, 2002.

Soil Survey Staff.: Soil survey laboratory information manual. Soil survey investigations report No. 45, version 2.0.  
 R. Burt (ed.). U.S. Department of Agriculture, Natural Resources Conservation Service.  
<https://www.nrcs.usda.gov/sites/default/files/2022-10/SSIR45.pdf>, 2011.

Song, X.X., Wang, P., van Z, L., Bolan, N., Wang, H.L., Li, X.M., Cheng, K., Yang, Y., Wang, M., Liu, T.X., and Li,  
 F.B.: Towards a better understanding of the role of Fe cycling in soil for carbon stabilization and  
 degradation, *Carbon Research*, 1, 5, <https://doi.org/10.1007/s44246-022-00008-2>, 2022.

Tokarski, D., Kučerík, J., Kalbitz, K., Demyan, M.S., Merbach, I., Barkusky, D., Ruehlmann, J., and Siewert, C.:  
 Contribution of organic amendments to soil organic matter detected by thermogravimetry, *J. Plant Nutr.*  
*Soil Sci.*, 181, 664-674, <https://doi.org/10.1002/jpln.201700537>, 2018.

Vithana, C.L., Sullivan, L.A., Burton, E.D., and Bush, R.T.: Stability of schwertmannite and jarosite in an acidic la  
 ndscape: Prolonged field incubation, *Geoderma*, 239-240, 47-57, <https://doi.org/10.1016/j.geoderma.2014.09.022>, 2015.

Volkov, D.S., Rogova, O.B., Proskurnin, M.A., Farkhodov, Y.R., and Markeeva, L.B.: Thermal stability of organic  
 matter of typical chernozems under different land uses, *Soil Till. Res.*, 197, 104500,  
<https://doi.org/10.1016/j.still.2019.104500>, 2020.

Wang, S.B., Hu, K.L., Feng, P.Y., Wei, Q., and Leghari, S.J.: Determining the effects of organic manure substitution  
 on soil pH in Chinese vegetable fields: a meta-analysis, *J. Soil. Sediment*, 23, 118-130,  
<https://doi.org/10.1007/s11368-022-03330-9>, 2023.

Wang, P., Wang, J., and Zhang, H.: The role of iron oxides in the preservation of soil organic matter under long-term  
 fertilization. *J. Soils Sediments* 19, 588–598. <https://doi.org/10.1007/s11368-018-2085-1>, 2019.

Wu, J.J., Zhang, H., Pan, Y.T., Cheng, X.L., Zhang, K.R., and Liu G.H.: Particulate organic carbon is more sensitive  
 to nitrogen addition than mineral-associated organic carbon: A meta-analysis, *Soil Till. Res.*, 232, 105770,  
<https://doi.org/10.1016/j.still.2023.105770>, 2023.

Yan, X., Zhou, H., Zhu, Q.H., Wang, X.F., Zhang, Y.Z., Yu, X.C., and Peng, X.H.: Carbon sequestration efficiency  
 in paddy soil and upland soil under long-term fertilization in southern China, *Soil Till. Res.*, 130, 42-51,  
<https://doi.org/10.1016/j.still.2013.01.013>, 2013.

Zhang, J.C., Zhang, L., Wang, P., Huang, Q.W., Yu, G.H., Li, D.C., Shen, Q.R., and Ran, W.: The role of non-  
 crystalline Fe in the increase of SOC after long-term organic manure application to the red soil of southern  
 China, *Eur. J. Soil Sci.* 64, 797-804, <https://doi.org/10.1111/ejss.12104>, 2013.

Zhang, B.Y., Dou, S., Guo, D., and Guan, S.: Straw inputs improve soil hydrophobicity and enhance organic carbon  
 mineralization, *Agronomy*, 13, 2618, <https://doi.org/10.3390/agronomy13102618>, 2023.

Zhou, P., Pan, G.X., Spaccini, R., and Piccolo, A.: Molecular changes in particulate organic matter (POM) in a typical  
 Chinese paddy soil under different long-term fertilizer treatments, *Eur. J. Soil Sci.*, 61, 231-242,

667 <https://doi.org/10.1111/j.1365-2389.2009.01223.x>, 2010.

668 Zhou, H., Fang H., Zhang, Q., Wang, Q., Chen, C., Mooney, S. J., Peng X.H., and Du, Z. L.: Biochar enhances soil  
669 hydraulic function but not soil aggregation in a sandy loam, *Eur. J. Soil Sci.*, 70, 291-300,  
670 <https://doi.org/10.1111/ejss.12732>, 2019.

671 Zou, Z.C., Ma, L.X., Wang, X., Chen, R.R., Jones, D.L., Bol, R., Wu, D., and Du, Z.L.: Decadal application of  
672 mineral fertilizers alters the molecular composition and origins of organic matter in particulate and  
673 mineral-associated fractions, *Soil Biol. Biochem.*, 182, 109042,  
674 <https://doi.org/10.1016/j.soilbio.2023.109042>, 2023.

675

676

**Table 1**

Soil organic carbon (SOC), total nitrogen (TN), the ration of SOC to TN (SOC/TN), pH, crystalline iron oxides (Fed), non-crystalline iron oxides (Feo), aggregate size distribution and mean weight diameter (MWD) of water-stable aggregates under no manure (Control), low manure (LM), high manure (HM) and high manure plus lime (HML) treatments.

Treatments	SOC (g kg <sup>-1</sup> )	TN (g kg <sup>-1</sup> )	SOC/TN	pH	Fed (g kg <sup>-1</sup> )	Feo (g kg <sup>-1</sup> )	Aggregate size distribution (g g <sup>-1</sup> )			MWD (mm)
							>0.25 mm	0.05-0.25 mm	<0.05 mm	
Control	4.79c	0.67c	7.10b	4.80c	62.99a	1.81b	0.67c	0.28a	0.05a	0.98b
LM	7.91b	1.00b	7.94a	5.42c	59.98a	1.74b	0.71b	0.25a	0.04ab	1.09b
HM	10.37a	1.35a	7.69ab	6.11b	59.59a	2.25a	0.77a	0.19b	0.03b	1.22a
HML	10.86a	1.40a	7.76ab	7.08a	62.22a	2.29a	0.78a	0.18b	0.04ab	1.32a

Values are the means (n=3). Different lowercase letters after values in the same row indicate a significant difference among four manure treatments ( $P < 0.05$ ). Fed: crystalline oxides; Feo: non crystalline oxides.

**Table 2**

Mass proportion, SOC concentration and contribution of the mineral-associated organic matter (MAOM) (<53 µm) fraction, particulate organic matter (POM) (>53 µm) fraction under no manure (Control), low manure (LM), high manure (HM) and high manure plus lime (HML) treatments.

Treatments	Mass proportion (%)		SOC concentration (g C kg <sup>-1</sup> soil)		Contribution to total SOC/%	
	MAOM	POM	MAOM	POM	MAOM	POM
Control	74.3a	16.6b	4.18c	0.44c	82.4a	8.8c
LM	75.1a	17.2ab	5.61b	1.26b	71.0b	15.9b
HM	73.9a	19.4a	6.81a	2.46a	65.8b	23.7a
HML	72.5a	19.3a	7.09a	2.84a	65.4b	26.0a

Values are the means (n=3). Different lowercase letters after values in the same row indicate a significant difference among four manure treatments ( $P < 0.05$ ). Calculations follow the methodology described in Section 2.4.

**Table 3**

The contents of various C functional groups in CPMAS-<sup>13</sup>C-NMR spectra under no manure (Control), low manure (LM), high manure (HM) and high manure plus lime (HML) treatments. Alkyl (0-45 ppm); O-alkyl C (45-110 ppm); aromatic C (110-160 ppm) and carbonyl C (160-220 ppm).

Treatments	alkyl C (%)	O-alkyl C (%)	aromatic C (%)	carbonyl C (%)	alkyl C/O-alkyl C	aromaticity (%)	aromatic C/O-alkyl C	aliphatic C/aromatic C	aliphaticity (%)
Control	25.4b	44.9c	15.3a	14.4a	0.57a	17.9a	0.34a	4.58b	82.1b
LM	26.2ab	47.4a	13.3b	13.1b	0.55b	15.3b	0.28b	5.53a	84.7a
HM	26.6a	46.1b	13.4b	13.9ab	0.58a	15.6b	0.29b	5.41a	84.4a
HML	26.5a	45.9b	13.3b	14.3a	0.58a	15.6b	0.29b	5.43a	84.4a

Values are the means (n=3). Different lowercase letters after values in the same row indicate a significant difference among four manure treatments ( $P < 0.05$ ). Aromaticity = aromatic C / (alkyl C + O-alkyl C + aromatic C); aliphatic C = (alkyl C + O-alkyl C); aliphaticity = (alkyl C + O-alkyl C) / (alkyl C + O-alkyl C + aromatic C).

**Table 4**

The mass losses during specific temperature ranges under no manure (Control), low manure (LM), high manure (HM) and high manure plus lime (HML) treatments. Exo<sub>1</sub> represents thermally labile soil organic matter (SOM); Exo<sub>2</sub> represents thermally stable SOM; Exo<sub>tot</sub> represents total SOM. TG-T<sub>50</sub> indicates the temperature at which half of the total SOM is lost.

Treatments	Exo <sub>1</sub> (180~380°C) (%)	Exo <sub>2</sub> (380~530°C) (%)	Exo <sub>tot</sub> (180~530°C) (%)	Exo <sub>1</sub> /Exo <sub>tot</sub>	TG-T <sub>50</sub> (°C)
Control	2.28c	2.36b	4.64b	0.49b	381a
LM	2.62b	2.54a	5.16a	0.51a	376ab
HM	2.69ab	2.68a	5.37a	0.50b	369b
HML	2.89a	2.56a	5.45a	0.53a	371b

Values are the means (n=3). Different lowercase letters after values in the same row indicate a significant difference among four manure treatments ( $P < 0.05$ ).



### Figure legends

**Fig. 1** CPMAS-<sup>13</sup>C-NMR spectra under no manure (Control), low manure (LM), high manure (HM) and high manure plus lime (HML) treatments. Alkyl (0-45 ppm); O-alkyl C (45-110 ppm); aromatic C (110-160 ppm) and carbonyl C (160-220 ppm)

**Fig. 2** Thermogravimetry (TG) curves (a) and corresponding derivative thermogravimetry (DTG) curves (b) of soil organic matter (SOM) under no manure (Control), low manure (LM), high manure (HM) and high manure plus lime (HML) treatments

**Fig. 3** The relationships between SOC and variables related to the chemical protection and physical protection

**Fig. 4** Relationship between soil pH and iron oxides concentrations.

**Fig. 5** Biplots of the principal component analysis (PCA) between the quantity and quality of SOC and variables related to chemical protection, physical protection across four manure application treatments (CK, Control; LM, low manure; HM, high manure; and HML, high manure plus lime)

**Fig. 6** The relationships between SOC quantity, chemical recalcitrance and thermal stability

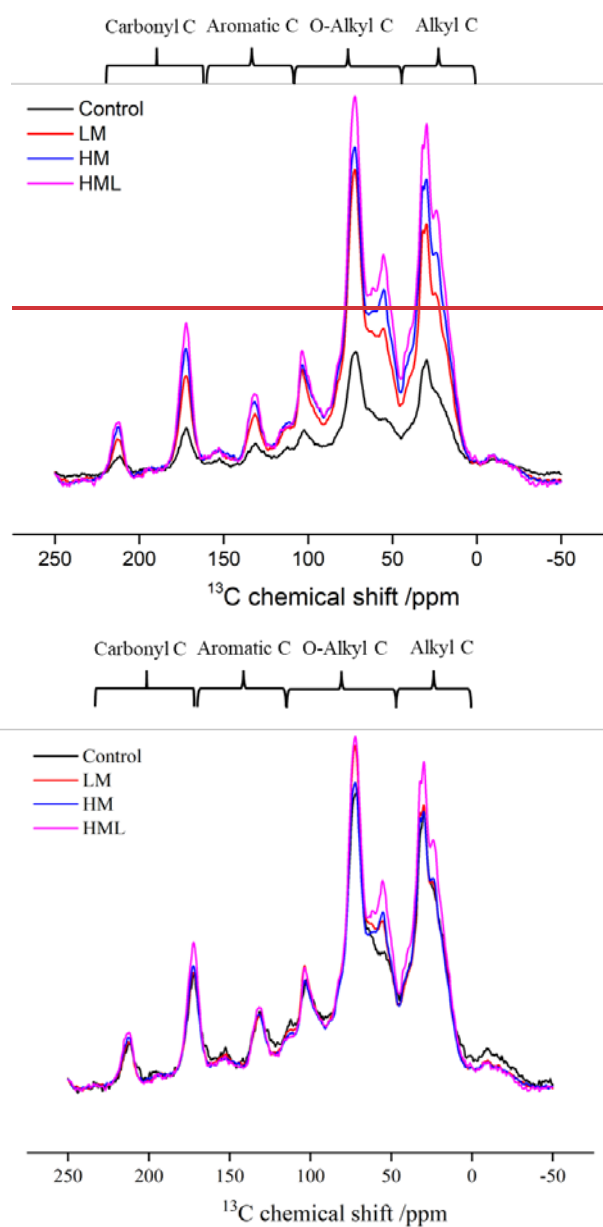


**Fig.1** CPMAS-<sup>13</sup>C-NMR spectra under no manure (Control), low manure (LM), high manure (HM) and high manure plus lime (HML) treatments. Alkyl (0-45 ppm); O-alkyl C (45-110 ppm); aromatic C (110-160 ppm) and carbonyl C (160-220 ppm). The spectra are normalized to the total integral area of the control spectrum to highlight differences in the relative abundances of carbon functional groups.

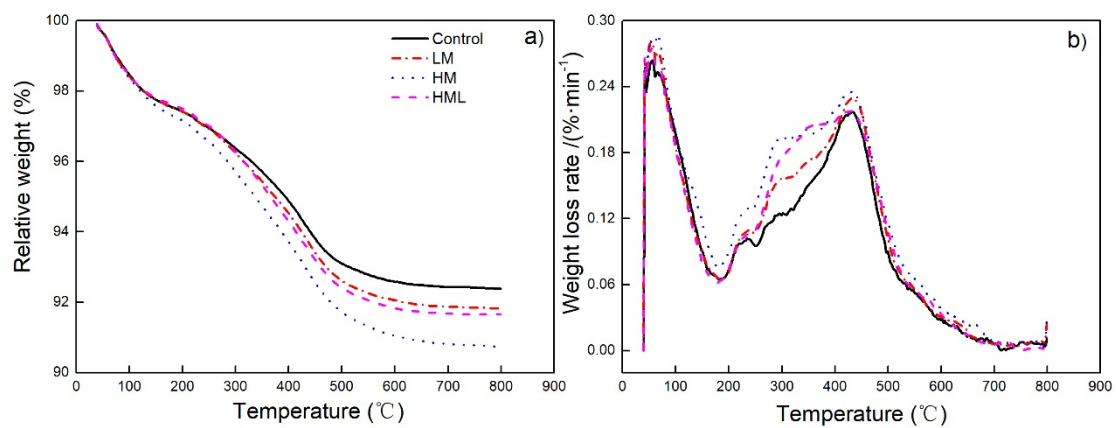


**Fig. 2** Thermogravimetry (TG) curves (a) and corresponding derivative thermogravimetry (DTG) curves (b) of soil organic matter (SOM) under no manure (Control), low manure (LM), high manure (HM) and high manure plus lime (HML) treatments

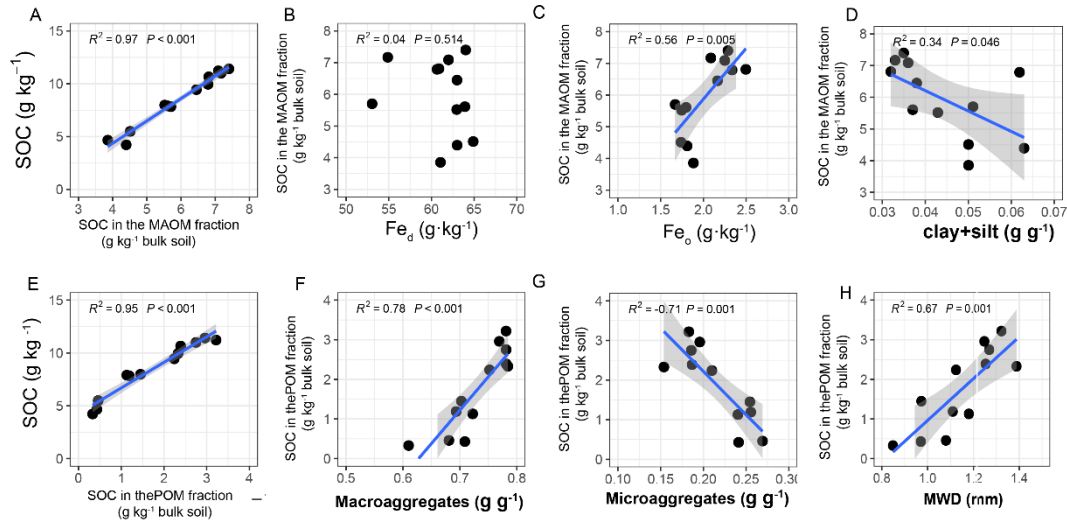


**Fig. 3** The relationships between SOC and variables related to the chemical protection and physical protection. (A to D) Variables characterizing chemical protection, including the content of SOC stored in the MAOM fraction, the content of crystalline Fe oxides (Fe<sub>a</sub>), the content of non-crystalline Fe oxides (Fe<sub>o</sub>), and the content of clay and silt. (E to H) Variables characterizing physical protection, including the content of SOC stored in the POM fractions, the content of soil macroaggregates, the content of soil microaggregates and the mean weight diameter (MWD)

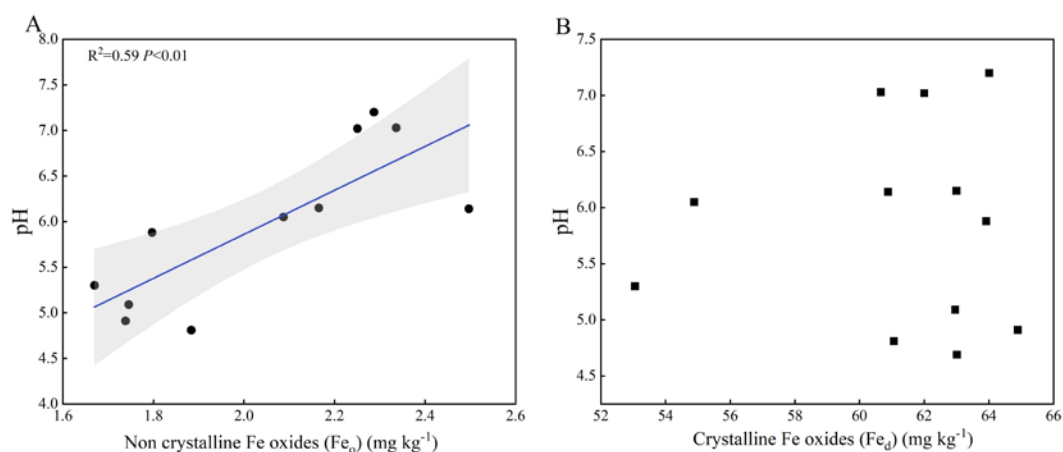


**Fig. 4** Relationship between soil pH and iron oxides concentrations. (A) Significant positive correlation between pH and amorphous iron oxides ( $\text{Fe}_o$ ). (B) No significant correlation between pH and crystalline iron oxides ( $\text{Fe}_d$ ).

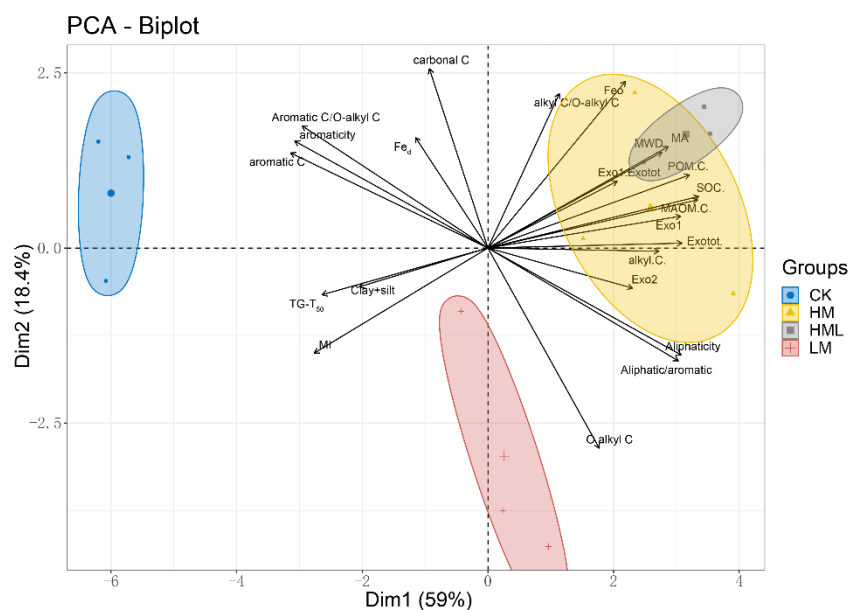


**Fig. 54** Biplots of the principal component analysis (PCA) between the quantity and quality of SOC and variables related to chemical protection, physical protection across four manure application treatments (CK, Control; LM, low manure; HM, high manure; and HML, high manure plus lime).  $Fe_d$ , crystalline Fe oxides;  $Fe_o$ , non-crystalline Fe oxides; MA, macroaggregates ( $>0.25$  mm); MI, microaggregates (0.05-0.25 mm); MWD, mean weight diameter; aromaticity, aromatic C / (alkyl C + O-alkyl C + aromatic C); aliphatic C, Alkyl C + O-alkyl C; aliphaticity, (Alkyl C + O-alkyl C) / (Alkyl C + O-alkyl C + Aromatic C);  $Exo_1$ , thermally labile soil organic matter (SOM);  $Exo_2$ , thermally stable SOM;  $Exo_{tot}$ , total SOM;  $TG-T_{50}$ , the temperature at which half of the total SOM was lost

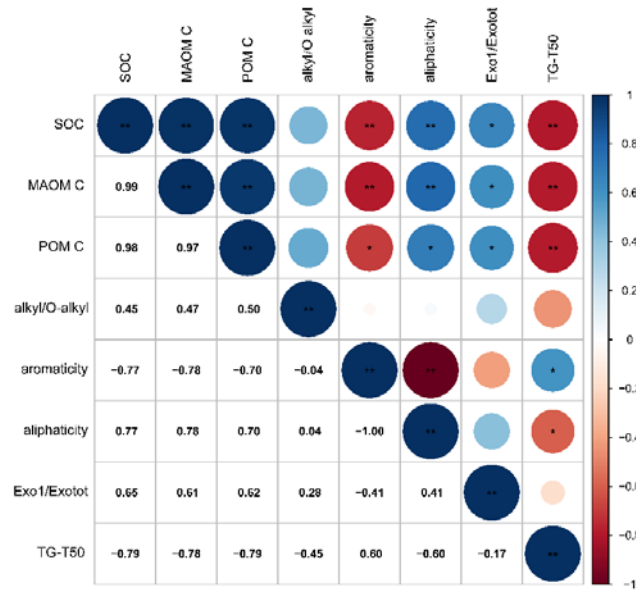


**Fig. 65** The relationships between SOC quantity, chemical recalcitrance and thermal stability. Aromaticity, aromatic C / (alkyl C + O-alkyl C + aromatic C); aliphaticity, (alkyl C + O-alkyl C) / (alkyl C + O-alkyl C + aromatic C); Exo<sub>1</sub>, thermally labile soil organic matter (SOM); Exo<sub>tot</sub>, total SOM; TG-T<sub>50</sub>, the temperature at which half of the total SOM was lost